

ASSEMBLY OF THE OUTER GALACTIC STELLAR HALO IN THE HIERARCHICAL MODEL

GIUSEPPE MURANTE

Osservatorio di Torino, Strada Osservatorio 20, I-10025, Pino Torinese (TO), Italy

EVA POGGIO

Dipartimento di Fisica Generale “Amedeo Avogadro”, Università degli Studi di Torino, Via P. Giuria 1, I-10125, Torino (Italy)

ANNA CURIR

Osservatorio di Torino, Strada Osservatorio 20, I-10025, Pino Torinese (TO), Italy

AND

ÁLVARO VILLALOBOS

I.N.A.F., Osservatorio di Trieste, Via Tiepolo 11, I- 34131, Trieste, Italy

Draft version May 18, 2010

ABSTRACT

We provide a set of numerical N-body simulations for studying the formation of the outer Milky Way’s stellar halo through accretion events. After simulating minor mergers of prograde and retrograde orbiting satellite halo with a Dark Matter main halo, we analyze the signal left by satellite stars in the rotation velocity distribution. The aim is to explore the orbital conditions where a retrograde signal in the outer part of the halo can be obtained, in order to give a possible explanation of the observed rotational properties of the Milky Way stellar halo. Our results show that, for satellites more massive than $\sim 1/40$ of the main halo, the dynamical friction has a fundamental role in assembling the final velocity distributions resulting from different orbits and that retrograde satellites moving on low inclination orbits deposit more stars in the outer halo regions end therefore can produce the counter-rotating behavior observed in the outer Milky Way halo.

Subject headings: galaxies: kinematic and dynamics; Galaxy: halo; methods: numerical

1. INTRODUCTION

The Galactic halo has long been considered a single component. However, evidences in the past few decades have indicated that it may be more complex (Preston et al. 1991; Majewski 1992; Kinman et al. 1994; Carney et al. 1996; Chiba & Beers 2000; Kinman et al. 2007; Miceli et al. 2008). Recently Carollo et al. (2007) confirmed the existence of a two-components halo, analyzing a large sample of calibration stars from the Sloan Digital Sky Survey (SDSS) DR5 (Adelman-McCarty et al. 2007). According to Carollo et al. the Galactic halo consists of two overlapping structural components, an inner and an outer halo. These components exhibits different spatial density profiles, stellar orbits and stellar metallicities. In particular the inner-halo stars show a small (or zero) net prograde rotation around the center of the Galaxy. Outer halo stars possess a clear retrograde net rotation.

The theory of galaxy formation in a Lambda cold dark matter (LCDM) Universe predicts galactic stellar halos to be built from multiple accretion events starting from the first structures to collapse (White & Rees 1978; Searle & Zinn 1978). Halos, composed of both dark and baryonic matter, grow by merging with other halos. While the gas from mergers and accretions loses

its energy through cooling and settles into a disk, the non dissipative material (accreted stars and dark matter) form a halo around the Galaxy. In a LCDM universe, a dark matter halo big enough to host the Milky Way contains 300 ± 100 subhalos (Diemand et al. 2004) (such a large number of subhalos is related to the so-called “missing satellites problem”, Moore et al. 1999).

There is significant evidence of past accretions into the Milky Way (Yanny et al. 2003; Belokurov et al. 2007; Grillmair 2009), and therefore we will accept the scenario that the Milky Way halo has been formed by subhalos accretion and we focus on possible origin of a retrograde (counter-rotating) outer stellar halo, defined as the set of stars orbiting around the Galaxy at large distance from the disk plane, say $z \gtrsim 15$ kpc: Carollo et al. (2007) found that this distance separates the inner and the outer halo. It is expected that such halo is made of stars stripped from merging or disrupted satellites of low mass (Zolotov et al. (2009); for a detailed study of accreting events onto a Milky-Way like halo, see also Boylan-Kolchin et al. (2010)). However, from cosmological simulation, prograde and retrograde mergers are approximately equally likely (Sales et al. 2007; Read et al. 2008).

In order to determine if, and in what condition, we can obtain a retrograde signal in the stellar distribution in the outer halo, we simulate minor mergers of a satellite halo onto a main halo of Galactic mass, with a mass ratio $M_{\text{primary}}/M_{\text{satellite}} \sim 40$. We put the satellite on two orbits, one prograde and one retrograde. After the satel-

Electronic address: murante@oato.inaf.it
 Electronic address: epoggio@studenti.ph.unito.it
 Electronic address: curir@oato.inaf.it
 Electronic address: villalobos@oato.inaf.it

lite completes its merging/disruption process, we identify stars at distance larger than 15 kpc from the disk plane and simply analyze their rotation velocities. Our main finding is that a counter-rotating stellar halo naturally arises when minor mergers happen on orbits with a low inclination with respect to the disk plane.

The plan of the Letter is the following. In Section 2, we describe our simulations; in Section 3, we give our results on counter-rotating outer halo stars, and in Section 4 we draw our conclusions.

2. SIMULATIONS

We use a primary Dark Matter (DM) halo containing a stellar, rotating exponential disk. The DM halo has a NFW (Navarro et al. 1997) radial density profile, and a mass, radius and concentration appropriate for a Milky Way like DM halo at redshift $z = 0$. DM particles have velocities given by the local equilibrium approximation (Hernquist 1993). Into our halo, we embed a truncated stellar disk, having an exponential surface density law: $\rho_{\text{stars}} = \rho_0 \exp(-(r/r_0))$ where r_0 is the disk scale length, and ρ_0 is the surface central density. We obtain each disk particle's position using the rejection method by Press et al. (1986); the disk is in gravitational equilibrium with the DM halo (see Curir & Mazzei (1999) for further details). We choose for the minor merger satellite a mass ratio of ≈ 40 , similar to the estimated mass ratio of the LMC to the Milky Way halo. The satellite contains a stellar bulge, with a Hernquist radial density profile. We realized our DM+bulge satellite configuration as in Villalobos & Helmi (2008). All the physical parameters of our merger are listed in Table 1.

We simulated prograde mergers, in which a satellite co-rotates with respect to the disk spin, and retrograde ones with a counter-rotating satellite. We chose two orbits used in Read et al. (2008) for studying the thickening of the disk due to the same kind of minor merger: a low-inclination one, with a 10 degree angle with the disk plane, and a high inclination one with a 60 degree angle. Initially, the center of the primary halo stays in the origin of our coordinate system and the satellite is in $(x, y, z) = (80.0, 0.27, -15.2)$ kpc for the low-inclination orbit and $(15.0, 0.12, -26.0)$ kpc for the high-inclination one. The (x, y, z) components of the velocity of the satellite are, in the prograde case, $(6.3, -62.5, 0.35)$ km/s for the low-inclination orbit and $(-1.2, 80.1, 2.0)$ km/s for the high-inclination one. The retrograde orbits have the y-component of the velocity inverted.

The secondary has always a spin parameter $\lambda = 0$, where we define $\lambda = J/(\sqrt{2}MVR)$, with M being the mass inside a radius R and $V = GM/R$ the circular velocity, as in Bullock et al. (2001). We use simulations with a primary halo with a spin parameter $\lambda = 1$ (simulations “A”) and $\lambda = 0$ (simulations “B”). We assign the angular momentum to DM particles using a rigid body rotation profile. The angular momentum of DM particles is always aligned with that of the stellar disk.

Our primary halo has 10^6 DM particles inside the virial radius ($\sim 2.5 \cdot 10^6$ in total) and one million star particles in the exponential disk, with mass $M_{\text{DM}} = 10^6 M_{\odot}$ and $M_{\star} = 5.97 \times 10^4 M_{\odot}$ respectively. Our DM+Bulge secondary halo has $1.1 \cdot 10^5$ DM particles and 10^5 bulge star particles, with masses $M_{\text{sat}} = 1.95 \times 10^5 M_{\odot}$ and $M_{\text{bulge}} = 2.38 \times 10^4 M_{\odot}$.

We use a Plummer-equivalent gravitational softening length $\varepsilon = 0.5$ kpc, and $\varepsilon = 0.25$ kpc for bulge star particles. We run all our simulation using the public parallel Treecode GADGET2 (Springel 2005).

To test the convergence of our results with resolution, we re-run our set “A” with ten times more particles in the satellite halo. We also changed the spin parameter of primary and secondary halos, its radial distribution using the profile from Bullock (Bullock et al. 2001), and their coupling.

We analyze positions and kinematic of the bulge stars, once the satellite completes its merging with the primary halo ¹. We run all our simulations for $t = 4.63$ Gyrs, corresponding to ~ 16 dynamical timescales of the main halo.

3. RESULTS

In all cases, in our simulations the satellite is slowed down by dynamical friction exerted on it by both disk and halo particles. At the first pericenter, tidal forces deform the satellite, redistributing its particle's energy (violent relaxation), and strips away some stellar particles (tidal stripping). The process continues at each subsequent passage to the pericenter, until no recognizable self-gravitating structure is present anymore. Stripped star particles tracks the orbital pattern of the satellite. The spatial distribution of stars depends upon the dynamical history of the satellite to which they belonged, i.e., how quickly it loses its orbital energy, how strongly it gets disrupted by tidal forces, and how these effects modify the orbit itself during the merger process.

We rotate our coordinate system so that the stellar disk lies in the X-Y plane. The origin is in the disk center of mass. To detect a rotation signal in the outer halo stars, we simply took all the star particles initially belonging to our satellite, and having a coordinate $Z > 15$ kpc or $Z < -15$ kpc. We then calculate the rotation velocity of such particles in the disk plane.

3.1. Distributions of v_{ϕ}

In Figure 1, we show histograms of the rotation velocity obtained in the four simulations of the set A: the satellite is either co-rotating or counter-rotating with respect to the disk, and the orbit has either a low or a high inclination with respect to the disk plane. In the upper panels, we show histograms at the final time of our simulations; in the lower ones, we performed an average over five consecutive snapshots, (~ 100 Myr) to get rid of possible sampling effect on the particle orbits which can rise using a particular instant of time. We show both the distribution of stars from single simulations, and the one resulting from taking together star particles from prograde and retrograde orbits having the same initial inclination. The latter gives us a hint on the possible rotation signal origin in the case a similar number of prograde and retrograde minor accretion events happen during the formation history of a galaxy, under the hypothesis that their inclination is the same. It is immediately clear from the Figure that our couple of low inclination orbits show an excess of counter-rotating stars in the outer halo.

¹ We define a merger to be complete when the z coordinate of the CM of all satellite stars remains within 2 kpc from the initial disk plane.

TABLE 1

PROPERTIES OF MAIN AND SATELLITE HALOS. COLUMN 1: HALO. COLUMN 2: VIRIAL MASS, IN M_\odot ; HERE, WE REFER ALL OUR VIRIAL QUANTITIES TO AN OVERDENSITY OF 200 TIMES THE MEAN COSMIC DENSITY. COLUMN 3: VIRIAL RADIUS, IN KPC. COLUMN 4: NFW CONCENTRATION PARAMETER. COLUMN 5: TRUNCATION RADIUS OF THE MAIN HALO; THE SECONDARY HALO HAS AN EXPONENTIAL CUT-OFF IN DENSITY. COLUMN 6: DISK SCALE RADIUS (MAIN HALO ONLY). COLUMN 7: DISK TRUNCATION RADIUS, IN KPC. COLUMN 8: DISK STELLAR MASS, IN M_\odot . COLUMN 9: HERNQUIST SCALE RADIUS, IN KPC. COLUMN 10: MASS OF THE STELLAR BULGE, IN M_\odot .

Halo	M_{200}	R_{200}	C_{200}	R_{trunc}	r_0	r_{disk}	M_*	a_b	M_b
Main	10^{12}	165	7.5	1300	4	20	$5.7 \cdot 10^{10}$	-	-
Satellite	$2.4 \cdot 10^{10}$	47	8.54	-	-	-	-	0.709	$2.4 \cdot 10^9$

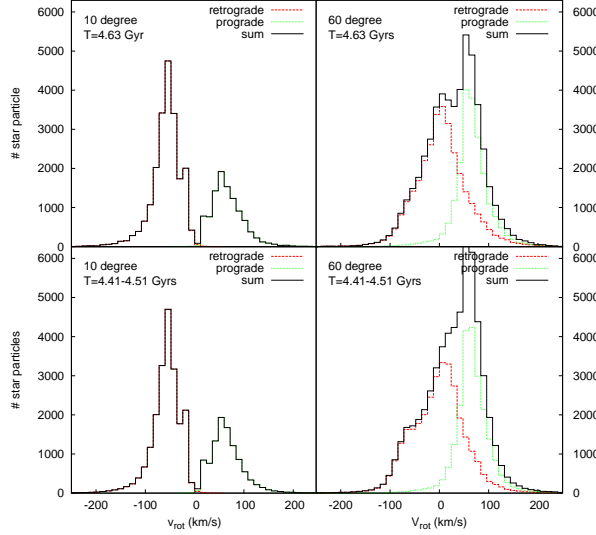


FIG. 1.— Histograms of rotation velocities for star particles in the outer halo, at the end of the set A of merger simulations. Upper panels show the histograms at the final time, lower panel show the same histograms, averaged over five simulation snapshots. In red (dashed line), we plot the histogram obtained for our retrograde orbits; in green (dotted line), those for our prograde orbits. In black (solid line) we show the sum of the two. Left column is for the low inclination orbits, right column for the high inclination ones. We used 50 velocity class, equispaced, between -300 and 300 km/s in all histograms.

Table 2 reports the number of satellite star particles in the positive and negative peak in all of our cases, and the number of particles having rotation velocity $v_{\text{rot}} < -10$ km/s and $v_{\text{rot}} > 10$ km/s. It also reports the same numbers obtained from our set B, in which the DM halo has no spin. We give such numbers for the final time of our simulations. The counter-rotating excess signal, defined as the fraction of the number of counter- to co-rotating satellite stellar particles, is 3.39 at peaks and 1.98 overall for the low-inclination orbits, while it is 1.3 (at peaks) for the high-inclination ones. Note that, for high-inclination orbits, the retrograde case shows a peak at a rotation velocity near to $v_{\text{rot}} = 0$. This is because high inclination orbits have a larger impact parameters. The disk responds by tilting more than in the low-inclination case, and as a result, rotation velocities in the disk reference frame are shifted towards more positive values. This effect is also present in our low-inclination runs, but it is much smaller because the tilt of the disk is smaller.

It remains to be determined if the counter-rotating signal is caused by the interaction with the stellar disk of

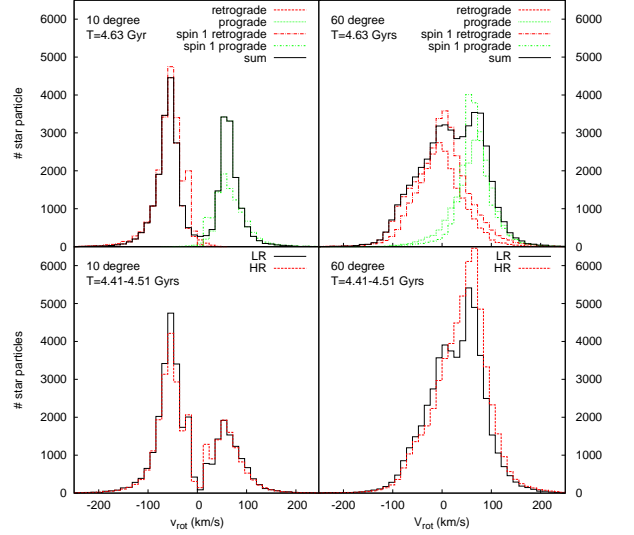


FIG. 2.— Upper row: histograms of rotation velocities for star particles in the outer halo, at the end of the set B of merger simulations, in which the main halo has no spin. In red (dashed line), we plot the histogram obtained for our retrograde orbits; in green (dotted line), those for our prograde orbits. In black (solid line) we show the sum of the two. Left panel is for the low inclination orbits, right panel for the high inclination ones. We also show the histogram for the case of spin 1 (dashed-dotted lines). Lower row: histogram of rotation velocities for star particles in the outer halo, for our set A, at the basic resolution (“LR”, black continuous line) and at a ten times better mass resolution (“HR”, red dashed line).

the main halo, or by the DM of the halo itself.

The upper row of Figure 2 shows the results of the same analysis performed on our set A, but in the case in which no halo spin is present (set B). Here we only show the results for our last snapshot; as in Figure 1, averaging over five snapshots makes no appreciable difference. Also in our set B, low inclination retrograde orbits produce more counter-rotating star particle than co-rotating stars produced by prograde orbits. Again, this is not the case for high inclination orbits. From Figure 2, it is clear that the excess of counter-rotating star is clearly smaller: and this is due to the fact that *more* co-rotating stars are produced by prograde orbit in our no spin case than in spin 1 case. From Table 2, the counter-rotating excess signal is 1.60 at peaks and 1.59 overall in the low inclination case, and 1.17 at peaks and 1.02 overall in the high inclination one.

Therefore, both disk rotation and halo spin contribute to the slowing-down of prograde orbits and to the consequent smaller amount of high-energy star particles

TABLE 2

NUMBER OF OUTER HALO SATELLITE STAR PARTICLES IN THE POSITIVE AND NEGATIVE PEAK IN ALL OF OUR CASES, AND THE NUMBER OF OUTER HALO SATELLITE STAR PARTICLES HAVING ROTATION VELOCITY $v_{\text{rot}} < -10$ km/s AND $v_{\text{rot}} > 10$ km/s IN OUR LOW INCLINATION RUN. RESULTS ARE FOR THE FINAL TIME OF OUR SIMULATIONS. FOR EACH INCLINATION, WE CONSIDERED TOGETHER PROGRADE AND RETROGRADE MERGERS. FIRST ROW: NUMBERS OF SATELLITE STAR PARTICLES HAVING ROTATION VELOCITIES SMALLER THAN -10 km/s OR HIGHER THAN 10 km/s, FOR THE LOW INCLINATION CASE. SECOND ROW: NUMBER OF STAR PARTICLE IN THE POSITIVE AND NEGATIVE PEAK, FOR THE LOW INCLINATION CASE. THIRD ROW: NUMBER OF STAR PARTICLES IN THE POSITIVE AND NEGATIVE PEAK, FOR THE HIGH INCLINATION CASE. SECOND COLUMN: NUMBER OF COUNTER-ROTATING SATELLITE STARS WHEN THE DM HALO HAS A SPIN $\lambda = 1$. THIRD COLUMN: NUMBER OF CO-ROTATING SATELLITE STARS WHEN THE DM HALO HAS A SPIN $\lambda = 1$. FOURTH COLUMN: NUMBER OF COUNTER-ROTATING SATELLITE STARS WHEN THE DM HALO HAS NO SPIN, $\lambda = 0$. FIFTH COLUMN: NUMBER OF CO-ROTATING SATELLITE STARS IN THE SAME $\lambda = 0$ CASES.

Distribution	$\lambda = 1$ counter	$\lambda = 1$ co	$\lambda = 0$ counter	$\lambda = 0$ co
10deg TOTAL $v_* > 10 $ km/s	20292	10237	16670	13033
10deg PEAK	6510 (-54)	1917 (+54)	4455 (-54)	3419 (54)
60deg PEAK	3581 (+6)	4010 (64)	2741 (-6)	3071 (78)

stripped from satellites that can reach the outer halo.

The lower row of Figure 2 shows that our result does not depend on the mass resolution of our satellite halo. Even using 10 times more particles in the secondary, only our low inclination couple of mergers shows an excess of counter-rotating stars in the outer halo.

3.2. Description of the mergers

Two effects are acting on the satellite halo in these kind of mergers: dynamical friction and tidal disruption. The first one is exerted both by the main halo DM particles and by the disk star particles. The second is most important near the center of the main halo, where the gravitational potential is stronger. But, dynamical friction depends upon the details of the satellite orbits. It is already known (Quinn & Goodman 1986; Walker et al. 1996; Huang & Carlberg 1997; Velazquez & White 1999; Villalobos & Helmi 2008) that prograde orbits tends to decay faster than retrograde ones. The dynamical friction *force* goes as $F_{\text{dyn}} \propto 1/v_s^2$ (Binney & Tremaine 2008), where v_s is the velocity of the satellite relative to the field particles; retrograde satellites have higher v_s with respect to prograde one, since in the first case the rotation velocity of the satellite is opposite to that of the disk and the main DM halo particles. Particles stripped from the satellites will remain on the orbit on which the satellite was when they were stripped. Therefore, retrograde satellites “deposit” more star particles in the outer halo regions, producing the signal we observe in our simulations, since their orbits have a longer decay time. Obviously, to obtain this effect, the *orbital* velocity must lie on the disk plane², which is almost the case for our low inclination orbits. High inclination encounters do not show such a behavior.

In Figure 3, we plot the position of the center of mass of all the star particles belonging to the satellite as a function of time. In our low inclination mergers (left panel), the prograde orbit decays faster: already after 1.5 Gyr, the difference with the behavior of the retrograde satellite is clear. In the high inclination cases the effect, though present, is much smaller, as expected.

We also verified that the effect we show here does not depend upon the exact angular momentum distribution

² DM spin is parallel to the disk spin: also the effect of the DM halo spin is maximum in such a case

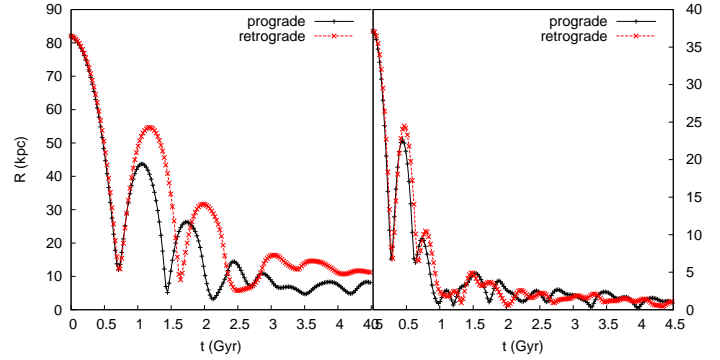


FIG. 3.— Position of the center of mass of all star particles belonging to the satellite, as a function of time. Left panel shows the result for our low inclination orbits, right panel for the high inclination ones. The center of mass position makes sense only until the satellite is not disrupted; this happens after ~ 3 Gyr in our low-inclination prograde simulation, ~ 4 Gyr in our low-inclination retrograde one, while in the high inclination cases the satellite is disrupted already after ~ 1 Gyr.

of particles in DM halo, by repeating our experiments using a Bullock (2001) profile instead of a rigid rotation one for the DM rotation velocity. Finally, the initial distance at which we put our satellite does not have a great impact on our results: we repeated the low-inclination mergers, putting the satellite at coordinates (29.5, 0.27, -5.2) kpc, thus much nearer to the center, and obtained the same qualitative behavior.

4. CONCLUSIONS

We performed controlled numerical simulations of minor merger events. Our aim was to determine if an excess of counter-rotating stars in the outer stellar halo can be produced by couples of mergers having orbits with identical inclination and opposite initial rotation. Our primary halo has an exponential stellar disk and its dark matter has a NFW radial density profile; our satellite’s DM has an NFW density profile, and contains a stellar spheroid with a Hernquist density profile. The mass ratio of our merger is $M_{\text{primary}}/M_{\text{satellite}} \sim 40$. We simulate low inclination encounters, in which the angle of the satellite’s

orbit with the disk plane is 10 degrees, and high inclination ones (60 degrees). We use prograde and retrograde orbits and also vary the DM spin parameter of the main halo. DM spin is aligned with the disk rotation. Here we define all stars having a distance $z > 15$ kpc from the disk plane as belonging to the outer stellar halo.

Our main results are the following:

- low inclination mergers do produce an excess of counter-rotating satellite stellar particles in the outer halo, independently on the spin of the DM;
- our 60 degrees mergers with our 1:40 mass ratio are not able to give a significant counter-rotating signal, also owing to the disk tilt produced by the merger itself;
- the fraction of counter-rotating to co-rotating satellite stars in the outer stellar halo is higher if the DM has spin.

From our controlled experiments, we now have an indication of the possible origin of the counter-rotation of stars observed in the Galactic outer halo in the context of a hierarchical Λ CDM model of galaxy formation, in which many major mergers happen during the history of the Galaxy. Even if, statistically, the number of prograde and retrograde minor merger is the same, still a counter-rotating signal can arise *if such mergers predominantly happen along low inclination orbits*. Since matter accretion, in a CDM dominated Universe, mainly occurs along filaments, this will be the case *if the galaxy*

disk is co-planar to the (majority of) filaments. The disk-filament alignment issue is still debated (see e.g. Brunino et al. 2007): from our results, we expect that if the galactic disk were perpendicular to the main accretion streams, no counter-rotating signal should be observed in the outer halo star distribution.

Our orbits are *not* cosmologically motivated, since the aim of our experiment is to determine *if* and *in what cases* an excess of counter-rotating stars in the outer halo can be produced. Of course, in a realistic case mergers will occur with orbits having a number of different inclinations, giving rise to a velocity distribution which will not show such a clear, double peaked signal as that detected in the present work. A detailed study of the orbital parameters of minor mergers in a statistically significant set of cosmological Galaxy-sized halo cosmological accretion histories is needed before a quantitative comparison between theory expectations and observation can be performed.

We acknowledge useful discussions with Daniela Carollo, Stefano Borgani, Gabriella De Lucia, Antonaldo Diaferio and Alessandro Spagna. The simulations were carried out at CASPUR, with CPU time assigned with the “Standard HPC grant 2009” call, and at the “Centro Interuniversitario del Nord-Est per il Calcolo Elettronico” (CINECA, Bologna), with CPU time assigned under an INAF/CINECA grant. A.C. acknowledge the financial support of INAF through the PRIN 2007 grant n. CRA 1.06.10.04 “The local route to galaxy formation”.

REFERENCES

- Adelman-McCarthy, J. K. et al, 2007, ApJS, 172, 634
 Belokurov, V. et al, 2006, ApJ, 642, L137
 Binney, J., & Tremaine, S., 2008, Galactic Dynamics: Second Edition, Princeton University Press, Princeton
 Boylan-Kolchin, M., Springel, V., White, S. D. M., Jenkins, A., 2009, arXiv/0911.4484
 Brunino, R., Trujillo, I., Pearce, F. R., & Thomas, P. A., 2007, MNRAS, 375, 184
 Bullock, J. S., Dekel, A., Kolatt, T. S., Kravtsov, A. V., Klypin, A. A., Porciani, C., & Primack, J. R., 2001, ApJ, 555, 240
 Carney, B. W., Laird, J. B., Latham, D. W., & Aguilar, L. A., 1996, AJ, 112, 668
 Carollo, D. et al., 2007, Nature, 450, 1020
 Chiba, M., & Beers, T. C., 2000, AJ, 119, 2843
 Curir, A., & Mazzei, P., 1999, A&A, 352, 103
 Diemand, J., Moore, B., & Stadel, J., 2004, MNRAS, 352, 535
 Grillmair, C. J., 2009, ApJ, 693, 1118
 Hernquist, L., 1993, ApJS, 86, 389
 Huang, S., & Carlberg, R. G., 1997, ApJ, 480, 503
 Kinman, T. D., Suntzeff, N. B., & Kraft, R. P., 1994, AJ, 108, 1722
 Kinman, T. D., Cacciari, C., Bragaglia, A., Buzzoni, A., & Spagna, A.
 Majewski, S. R., 1992, ApJS, 78, 87
 Miceli, A. et al., 2008, ApJ, 678, 865
 Moore, B., Ghigna, S., Governato, F., Lake, G., Quinn, T., Stadel, J., & Tozzi, P., 1999, ApJ, 524, L19
 Navarro, J. F., Frenk, C. S., & White, S. D. M.
 Press, W. H., Flannery, B. P., & Teukolsky, S. A., 1986, Numerical recipes. The art of scientific computing, Cambridge: University Press, 1986
 Preston, G. W., Shectman, S. A., & Beers, T. C., 1991, ApJ, 375, 121
 Quinn, P. J., & Goodman, J., 1986, ApJ, 309, 472
 Read, J. I., Lake, G., Agertz, O., & Debattista, V. P., 2008, MNRAS, 389, 1041
 Sales, L. V., Navarro, J. F., Abadi, M. G., Steinmetz, M., 2007, MNRAS, 379, 1464
 Searle, L., & Zinn, R., 1978, ApJ, 225, 357
 Springel, V., 2005, MNRAS, 364, 1105
 Velazquez, H., & White, S. D. M., 1999, MNRAS, 304, 254
 Villalobos, Á., & Helmi, A., 2008, MNRAS, 391, 1806
 Walker, I. R., Mihos, J. C., & Hernquist, L., 1996, ApJ, 460, 121
 White, S. D. M., & Rees, M. J., 1978, MNRAS, 183, 341
 Yanny, B. et al., 2003, ApJ, 588, 824
 Zolotov, A., Willman, B., Brooks, A. M., Governato, F., Brook, C. B., Hogg, D. W., Quinn, T., & Stinson, G., 2009, ApJ, 702, 1058